NASA TECHNICAL NOTE

NASA TN D-7628

NASA TN D-7628

OXIDATIVE VAPORIZATION KINETICS OF CHROMIUM (III) OXIDE IN OXYGEN FROM 1270 TO 1570 K

by Carl A. Stearns, Fred J. Kohl, and George C. Fryburg

Lewis Research Center
Cleveland, Ohio 44135

NATIONAL AERONAUTICS AND SPACE ADMINISTRATION • WASHINGTON, D. C. • MAY 1974

1. Report No.	2. Government Accession No.	3. Recipient's Catalog No.
NASA TN D-7628		

4. Title and Subtitle	5. Report Date
OXIDATIVE VAPORIZATION KINETICS OF CHROMIUM (III) OXIDE IN OXYGEN FROM 1270 TO 1570 K	May 1974
	6. Performing Organization Code
7. Author(s)	8. Performing Organization Report No.
Carl A. Stearns, Fred J. Kohl, and George C. Fryburg	E-7788
	10. Work Unit No.
9. Performing Organization Name and Address	502-01
Lewis Research Center National Aeronautics and Space Administration Cleveland, Ohio 44135	11. Contract or Grant No.
	13. Type of Report and Period Covered
12. Sponsoring Agency Name and Address	Technical Note
National Aeronautics and Space Administration Washington, D.C. 20546	14. Sponsoring Agency Code

15. Supplementary Notes

16. Abstract

Rates of oxidative vaporization of Cr_2O_3 on preoxidized resistively heated chromium were determined in flowing oxygen at a pressure of 15.3 N m^{-2} (0.115 torr) for temperatures from 1270 to 1570 K. Reaction-controlled rates were obtained from experimental rates by a gold calibration technique. These rates were shown to agree with those predicted by thermochemical analysis. The activation energy obtained for the oxidative vaporization reaction corresponded numerically with the thermochemical enthalpy of the reaction. A theoretical equation is given for calculating the rate from thermodynamic data by using boundary-layer theory.

17. Key Words (Suggested by Author(s))	18. Distribution Statement
Oxidation; Vaporization; Kinetics; Chromium; Chromium oxides; Thermodynamics; Activation energy	Unclassified - unlimited Category 06

19. Security Classif. (of this report)	20. Security Classif. (of this page)	21. No. of Pages	22. Price*
Unclassified	Unclassified	23	$3.00

* For sale by the National Technical Information Service, Springfield, Virginia 22151

OXIDATIVE VAPORIZATION KINETICS OF CHROMIUM (III) OXIDE IN OXYGEN FROM 1270 TO 1570 K *

by Carl A. Stearns, Fred J. Kohl, and George C. Fryburg

Lewis Research Center

SUMMARY

Rates of oxidative vaporization of chromium (III) oxide (Cr_2O_3) on preoxidized resistively heated chromium were determined in flowing oxygen at a pressure of 15.3 N m^{-2} (0.115 torr) for temperatures from 1270 to 1570 K. Reaction-controlled rates were obtained from experimental rates by a gold calibration technique. These rates were shown to agree with those predicted by thermochemical analysis. The activation energy obtained for the oxidative vaporization reaction corresponded numerically with the thermochemical enthalpy of the reaction. A theoretical equation is given for calculating the rate from thermodynamic data by using boundary-layer theory.

INTRODUCTION

Numerous investigators have studied the kinetics of chromium (III) oxide (Cr_2O_3) scale formation on chromium and chromium-containing alloys heated in oxidizing environments (refs. 1 to 8). Gravimetric measurements above 1270 K yield a net weight loss which has been shown to be caused by the loss of the gaseous species chromium (VI) oxide (CrO_3) formed from the reaction of the Cr_2O_3 protective scale with oxygen (ref. 3). The volatilization of CrO_3 has been incorporated into the analyses of the kinetics of oxidation of materials with Cr_2O_3 scales (refs. 7 and 9). However, Caplan and Cohen (ref. 5), Hagel (ref. 3), and Graham and Davis (ref. 10) appear to be the only investigators to have measured explicitly the oxidative vaporization of Cr_2O_3.

Caplan and Cohen (ref. 5) established that CrO_3 was the species which accounted for the evaporation of chromium oxide when Cr_2O_3 was heated in oxygen, although they

---

* An abbreviated account of this work was presented as a technical paper at the 144th Meeting of the Electrochemical Society, Boston, Mass., Oct. 7 to 11, 1973, Abstract No. 105.

did not identify CrO_3 in the vapor phase. Grimley, Burns, and Inghram (ref. 11) subsequently identified this molecule in the vapor phase by mass spectrometry. Hagel (ref. 3) measured the rate of weight loss of Cr_2O_3 heated in oxygen and obtained a vaporization-temperature relation which he used to correct his scale formation data. Hagel's vaporization corrections may be valid for his data obtained in a single experimental arrangement. However, his vaporization data cannot be considered as valid for other experimental arrangements (refs. 6 and 7) because the volatilization reaction was undoubtedly gas diffusion controlled under the conditions of his experiments (furnace tests with static oxygen pressure of 1.0×10^4 N m^{-2} (76 torr)). The danger in using furnaces to study reactions that yield volatile products has been explained by Fryburg and Murphy (ref. 12). Experimental techniques required to obtain meaningful data for such reactions have been described by Fryburg and Petrus (refs. 13 and 14) for the oxidation of platinum. They showed that above a certain gas pressure (dependent on sample size and geometry) oxidative vaporization reactions become limited by mass transport through a boundary layer. Bartlett (refs. 15 and 16) has developed mass transport equations which adequately explain experimental results over a wide range of temperature, pressure, and flow rate for the oxidation of both platinum and tungsten. Considerations such as these must be applied when studying the oxidative vaporization of Cr_2O_3.

Recently, Graham and Davis (ref. 10) investigated the oxidative vaporization of hot-pressed and sintered samples of Cr_2O_3 in free and forced convection in the pressure range 1.0×10^2 to 1.0×10^5 N m^{-2} (10^{-3} to 1 atm). They properly treated the mass transport problem and showed that the total pressure and flow dependencies were consistent with the assumption that the rate-controlling step was the diffusion of CrO_3(g) through a stagnant boundary layer. However, this study was made only at 1473 K, and rates were not measured in the reaction-controlled regime.

The work reported herein was undertaken to determine the rate of oxidative vaporization of Cr_2O_3(s) in molecular oxygen and its dependence on temperature. This work is part of a study of the enhanced oxidation of Cr_2O_3 and chromium produced by exposure to oxygen atoms (ref. 17). The experimental arrangement used in the program was dictated by requirements of the oxygen atom study. While this arrangement did not lend itself to a simple theoretical mass transport analysis, meaningful rate data were obtained by the use of a gold calibration technique.

MATERIALS, APPARATUS, AND PROCEDURE

Samples

Test samples (12 cm long by 0.3 cm wide and 0.04 cm thick) were prepared from a chromium - 0.1-weight-percent yttrium alloy made from iodide chromium by arc melt-

ing and drop casting into a water-cooled copper mold. A small yttrium addition improves oxide adherence. Samples were diamond sawed from hot-rolled sheet of the alloy. Sample surfaces were cleaned with a dental abrasive unit (using 50-μm alumina powder and nitrogen gas) and anodically electropolished in a 2-percent sodium hydroxide solution for 1 to 3 minutes with a current density of 0.3 A cm^{-2}. Prior to testing, samples were washed with hot water and rinsed in ethanol.

Emission spectrographic and chemical analysis of samples yielded the following typical impurity analysis in parts per million: 230 iron, 10 aluminum, 8 copper, 5 calcium, 2 magnesium, 60 carbon, 50 oxygen, 5 nitrogen, and 5 hydrogen.

Apparatus

A schematic diagram of the experimental apparatus is shown in figure 1. The sample was supported vertically by a fixed clamp at the top and a movable clamp at the bottom to allow for thermal expansion when the sample was heated. The bottom clamp was mounted in a linear ball bushing in such a fashion that it was free to move vertically but was constrained from rotating.

The test chamber was evacuated with two 425×10^{-3} m^3 min^{-1} mechanical pumps. A $400\times10^{-3}m^3$ sec^{-1} oil diffusion pump was also available for high vacuum pumping.

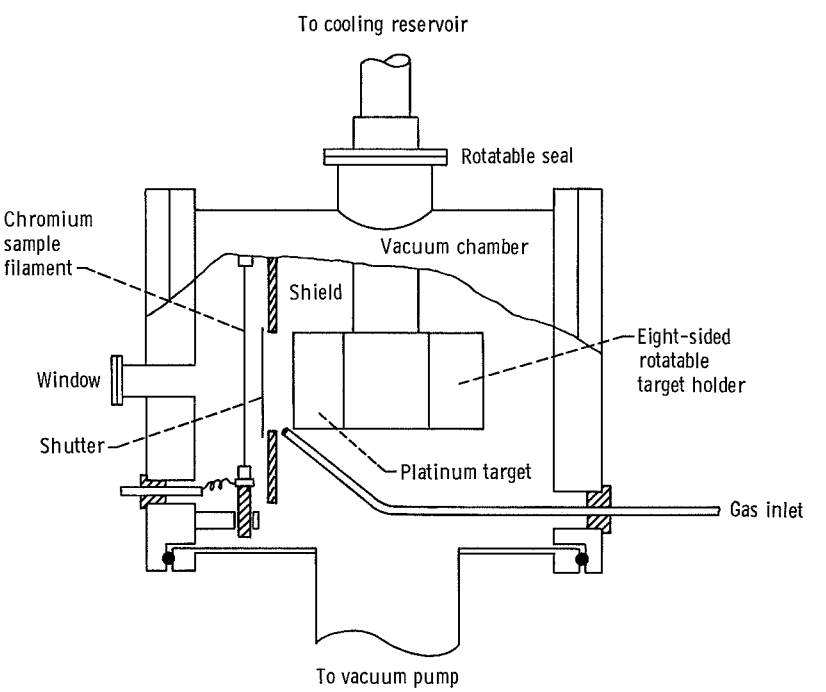

Figure 1. - Schematic diagram of experimental apparatus.

Gases were admitted into the system through a Pyrex tube (1.4 cm o.d.) connected to a flow control and a mixing manifold. The glass tube was arranged so that incoming gas impinged directly onto the flat side of the sample. Research-grade gases were used in all experiments.

Gas pressures in the test chamber were measured with a vacuum thermocouple gage; the filament was heated by a 30-milliampere current from a regulated direct-current power supply. Thermocouple voltages were read to the third decimal place with a digital voltmeter. The thermocouple gage was calibrated for oxygen against a McLeod gage. For other gases and gas mixtures, calibration was against a fused-quartz precision pressure gage.

Temperature control for the resistively heated sample was facilitated by a platinum/platinum - 13-percent rhodium thermocouple (0.127-mm-diameter wire) spot welded to the back face of the sample at its midpoint. This thermocouple was the primary element for a precision set-point, proportional controller-indicator. The output of the controller was used to drive a voltage-controlled 100-ampere direct-current power supply. The power supply output was fed to the sample through insulated, water-cooled feedthroughs and flexible copper braid.

For all experimental conditions the sample temperature was held constant with time to at least ±0.5 K. Temperatures were also measured with a micro-optical brightness pyrometer (λ = 650 nm) to supplement the thermocouple. The pyrometer was sighted through a shutterable window onto the back surface of the sample and the pyrometer-read temperatures were corrected for window absorption and sample emissivity. Corrected pyrometer temperatures measured next to the thermocouple junction were found to be in agreement with the thermocouple-indicated temperatures if a value of 0.7 was used for the sample emissivity. This value is consistent with literature values (ref. 18) for the emissivity of oxidized chromium.

The pyrometer was used mainly to survey the length of a sample for temperature gradients. Samples were discarded if the central portion opposite the opening to the collection target was not uniform in temperature to within ±5 K.

Products vaporizing from the sample passed through an opening (2.6 cm on a side) in a water-cooled copper shield and were condensed on a cooled platinum target. Eight targets (5.1 cm on a side and 0.125 mm thick) were clamped against an eight-sided copper mounting block by copper frames screwed to the block. The block in turn was attached to a cylindrical copper reservoir through which coolant was circulated. The whole assembly could be externally rotated relative to the sample so that a designated target could be brought into position opposite the sample. Targets not directly in front of the sample were masked from the sample by the copper shield. In addition, the opening in the shield could be closed with an externally controllable water-cooled shutter. The distance from the target to the sample was approximately 1.8 centimeters.

Ethanol was used as the coolant for the target assembly. The ethanol was cooled in

a dry-ice - alcohol bath. Tests were made prior to actual experiments to determine target temperature as a function of sample temperature and time. For these tests a thermocouple was attached to the face of a target facing the sample. These tests demonstrated that the target temperature could be held below 343 K for indefinite periods of time when the sample temperature was 1570 K. Lower sample temperatures yielded proportionately lower target temperatures.

Procedure for Cr_2O_3(s) Oxidations

Cleaned chromium samples were preoxidized in situ before an oxidation experiment by heating to the desired oxidation temperature for 1/2 hour in a 15.3 N m^{-2} (0.115 torr) of flowing oxygen. For the temperatures of the experiments (1270 to 1570 K), approximately 0.01-millimeter (0.4-mil) oxide scales were formed, as shown in figure 2.

Oxidation runs at each pressure and temperature were started by opening the shutter and collecting the diffusate on a target for a measured length of time. At 1270 K, runs extended for 8 to 10 hours per target; but at 1520 K, runs were only of the order of 10 minutes in length. Generally, between 5 to 25 micrograms of chromium were collected on a given target. After a series of runs (one for each of the eight targets) was

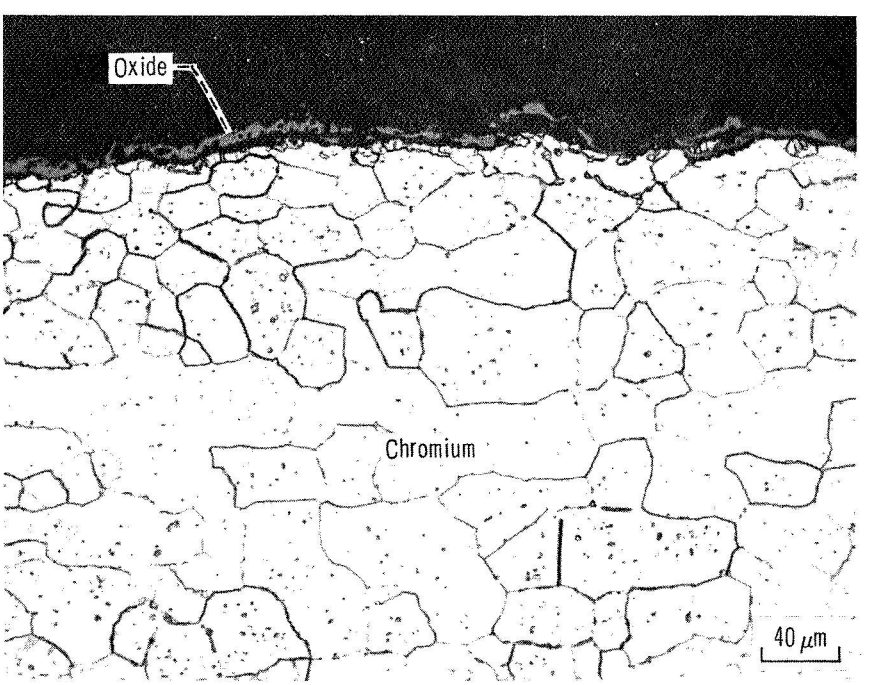

Figure 2. - Microstructure of typical oxidized specimen of Cr-0.1Y showing oxide scale. Etchant, 10 percent sulfuric acid/chromic acid.

completed, the sample was cooled and the block and targets were warmed to room temperature. Clean dry air was admitted to the system, and the targets were removed for condensate analysis. The condensate was dissolved from each target with a stream of distilled water, and the resulting solution was diluted to a measured volume. Each solution, corresponding to a designated target and run, was quantitatively analyzed for chromium content by atomic absorption spectroscopy. The spectrometer was calibrated with solutions prepared from a purchased standard potassium dichromate solution. The analysis method had a sensitivity of 0.02 part of chromium per million. Sample solutions were usually held in the range from 0.2 to 2 ppm.

Procedure for Gold Calibrations

In order to obtain reaction-controlled rates from our experimental rates, it is obvious that we must determine the fraction of the CrO_3 formed that is actually condensed on the target. This is called the "collection fraction" of the apparatus. In addition, the oxidative vaporization may be diffusion limited (refs. 12, 13, and 19). If so, we must determine the fraction of CrO_3 volatilizing from the specimen surface that diffuses through the boundary layer to the target. This is called the "escape fraction."

These two fractions were determined by measuring the rate of evaporation of gold ribbons in the apparatus. The gold was 99.99 percent pure, with silver and silicon being the major metallic impurities. The gold samples were the same length and width as the chromium samples, but the thickness was only 0.025 centimeter. Gold samples were cleaned in aqua regia and rinsed with water and ethanol.

The gold samples were mounted and heated in a manner identical to that used for the chromium samples. Because of the high thermal conductivity of gold, temperature gradients were unavoidable; usually a temperature drop of about 20 K existed over the length from midpoint to the top or bottom edge of the collection opening. Temperatures were measured with the optical pyrometer at 0.5-centimeter intervals over the 2.6-centimeter collection opening. Rates of evaporation were calculated and summed for 0.5-centimeter increments along the sample by using the average temperature of each increment.

Experimental runs were performed at temperatures around 1270 K under good vacuum conditions ($\sim 5\times10^{-6}$ torr) and under the conditions of the oxidation experiment with flowing oxygen at 5×10^{-3} m^3 hr^{-1} (STP) and 15.3 N m^{-2} (0.115 torr) pressure. Between 25 and 50 micrograms of gold were collected on each platinum target. The quantity of gold on each target was determined by dissolving the gold in a stream of concentrated nitric acid, diluting with water to a measured volume, and analyzing the solution by atomic absorption spectroscopy. The sensitivity of the gold analysis was 0.1 ppm and sample solutions were usually 1 to 2 ppm.

THERMOCHEMICAL PREDICTIONS

Fryburg and Petrus (ref. 13) showed that kinetic data, obtained from a study of the oxidative vaporization of platinum, could be correlated with equilibrium thermodynamic data. It is useful to reverse this process and to predict kinetic behavior from thermodynamic data. Kellogg-type (ref. 20) equilibrium thermochemical diagrams aid in such predictions, as demonstrated by Gulbransen and Jansson (refs. 21 to 24) for the chromium-oxygen system. Gulbransen and Jansson employed the free energy of formation ΔG_f^o and equilibrium constant $\log K_p$ data for the gaseous chromium-oxygen molecules CrO, CrO_2, and CrO_3 as compiled by Schick (ref. 25) from the original mass spectrometric studies of reference 11. The diagrams show that the important molecular species in equilibrium with Cr_2O_3(s) and O_2(g) should be CrO_3(g) and CrO_2(g) in the temperature range 1000 to 2000 K and at oxygen pressures greater than 10^{-1} N m^{-2} (10^{-6} atm). The results of a recent transpiration study of the Cr_2O_3-O_2 system by Kim and Belton (ref. 26), which apparently yielded more reliable data for CrO_3(g), were employed by Kohl and Stearns (refs. 27 and 28) to construct revised diagrams which showed that the CrO_3 molecules should be greater than an order of magnitude more abundant than indicated by Gulbransen and Jansson. Recent mass spectrometric studies on the vaporization of CrO_3(c) by Schäfer and Rinke (ref. 29), McDonald and Margrave (ref. 30), and Washburn (ref. 31) have established the existence of several "new" chromium oxide vapor species: $(CrO_3)_3$, $(CrO_3)_4$, $(CrO_3)_5$, Cr_3O_7, Cr_4O_{10}, and Cr_5O_{13}. In addition, Cr_2(g) has been identified by Kant and Strauss (ref. 32). Therefore, we have recalculated diagrams for the chromium-oxygen system and included the new vapor species.[1]

A thermochemical diagram at 1500 K is shown in figure 3. The diagram was constructed by the methods outlined by Gulbransen and Jansson (ref. 21). For O_2 pressures greater than 10^{-3} N m^{-2} (10^{-8} atm), CrO_3(g) is still the predominant vapor species above Cr_2O_3(s), but the new species Cr_3O_7(g) becomes more important than CrO_2(g) for O_2 pressures greater than 10^4 N m^{-2} (10^{-1} atm). As pointed out by Gulbransen and Jansson, Cr atoms are the predominant vapor species at the Cr(s) - Cr_2O_3(s) interface. The existence of the complex polymeric gaseous molecules is not unexpected if chromium is compared with the other Group VIIB metals, molybdenum (Mo) and tungsten (W). Gulbransen and Jansson (refs. 22 to 24, and 34) have constructed thermochemical diagrams for the molybdenum- and tungsten-oxygen systems which demonstrate that the

---

[1] Thermodynamic data for Cr(g), CrO(g), and CrO_2(g) were taken from Schick (ref. 25). Data for Cr_2O_3(s) were calculated from ΔG_f^o values given by Wicks and Block (ref. 33). Thermodynamic data for CrO_3(g) and the "new" chromium-oxygen molecules are given in reference 17.

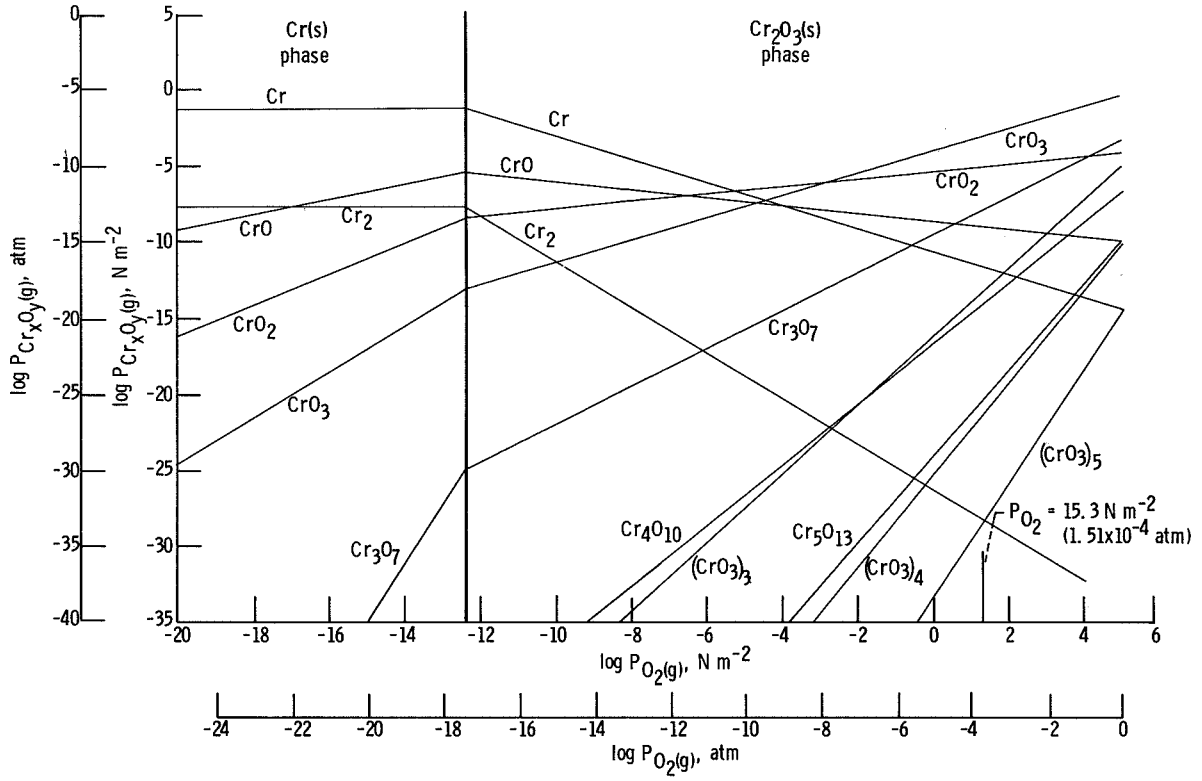

Figure 3. - Equilibrium thermochemical diagram for the chromium - molecular oxygen system at 1500 K.

complex molecular species $(MoO_3)_3$ and $(WO_3)_3$, $(WO_3)_4$, and W_3O_8, respectively, are the most abundant vapor species in equilibrium with the condensed-phase dioxide and trioxide at high oxygen pressures. The differences between chromium and molybdenum or tungsten are manifested in the existence of the stable Cr_2O_3 phase for chromium and the absence of a sesquioxide for molybdenum and tungsten where MoO_2 and MoO_3 and WO_2 and WO_3, respectively, are the stable condensed oxides. Chromium dioxide (CrO_2), chromium trioxide (CrO_3), and possibly other chromium-oxygen stoichiometries (ref. 35) can exist as metastable condensed phases at low oxygen pressures. At 1500 K the calculated equilibrium O_2 pressure at the Cr_2O_3-CrO_3 phase boundary is $10^{9.20}$ N m^{-2} ($10^{4.19}$ atm). Thus, if the log $P_{O_2(g)}$ axis of figure 3 were extended to higher values, the CrO_3(c) phase would be stable and the complex chromium-oxygen molecules would be the predominant vapor species.

The slope of the CrO_3(g) line in the Cr_2O_3(s) phase region is 3/4 and can be expected to describe the dependence of CrO_3(g) pressure on oxygen pressure (ref. 10).

From the respective diagrams at different temperatures, we can obtain the vapor pressures of each species as a function of temperature for any given oxygen pressure. Thus, in figure 4 we have plotted the vapor pressure of the major species over the

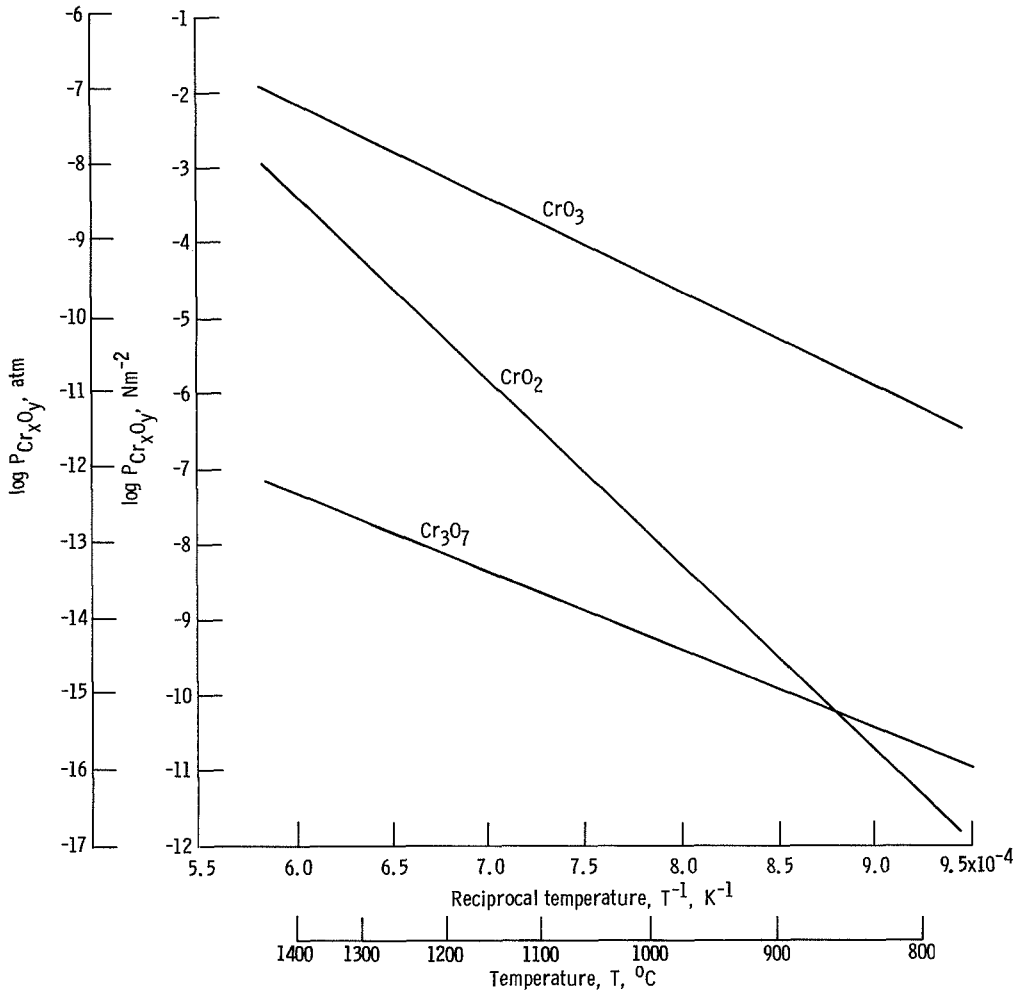

Figure 4. - Vapor pressure of the major species over the Cr_2O_3(s) phase as a function of reciprocal temperature. Oxygen pressure, P_{O_2}, 15.3 N m^{-2} (1.51×10^{-4} atm).

Cr_2O_3(s) phase, for an oxygen pressure of 15.3 N m^{-2} (1.51×10^{-4} atm), against reciprocal temperature. From this figure it is obvious that CrO_3(g) will be the major vapor product in the oxidative vaporization of Cr_2O_3(s) under our experimental conditions over the entire temperature range of this study. The slope of the CrO_3(g) line in figure 4 is related to the enthalpy change for the reaction

$$\frac{1}{2} Cr_2O_3(s) + \frac{3}{4} O_2(g) = CrO_3(g) \qquad (1)$$

In the case of the oxidative vaporization of platinum, the enthalpy change was shown to be equivalent to the energy of activation for the reaction (ref. 13). Thus, it is not unreasonable to expect the same kind of correlation in the present studies.

The vapor pressure of $CrO_3(g)$ can be expressed analytically as

$$\log P_{CrO_3(g)}(N\ m^{-2}) = \frac{-1.247\times10^4}{T} + 8.21 + \frac{3}{4}\log P_{O_2(g)}(N\ m^{-2}) \qquad (2)$$

over the temperature range 1270 to 1570 K, where the thermodynamic data[2] have been taken from the work of Kim and Belton (ref. 26). Using the Hertz-Langmuir equation and the vapor pressure of $CrO_3(g)$ from equation (2), we can calculate the rate of vaporization of $CrO_3(g)$ and/or the rate of loss of chromium caused by vaporization of the oxide. The rate of loss of chromium is given by

$$\dot{m}(g\,Cr\,cm^{-2}\,sec^{-1}) = P_{CrO_3(g)}\left(2\pi RTM_{CrO_3}\right)^{-1/2} M_{Cr}$$

$$= 4.377\times10^{-4}\,P_{CrO_3(g)}(N\ m^{-2})\,\frac{M_{Cr}}{\left(M_{CrO_3}\right)^{1/2}T^{1/2}} \qquad (3)$$

where M_i is the appropriate molecular weight. We have used this equation[3] to calculate the predicted maximum rate of oxidative vaporization of $Cr_2O_3(s)$. This rate corresponds to reaction-controlled conditions uninhibited by mass transport through a boundary layer.

RESULTS AND DISCUSSION

Preliminary Calibrations

Oxidative vaporization reactions obey linear kinetics, that is, the rates are independent of time. Preliminary experiments validated the time independence of the rates for

---

[2]The results of Kim and Belton (ref. 26) were obtained in a temperature range of 1600 to 1860 K. We have adjusted their vapor pressure expression to our temperature range by use of the heat contents of $CrO_3(g)$, $O_2(g)$, and $Cr_2O_3(s)$.

[3]This equation is slightly different from that given previously by Kohl and Stearns (refs. 27 and 28) and Rapp (ref. 36). The previous equation was not dimensionally correct and yielded results about 40 percent too high.

the oxidative vaporization of Cr_2O_3. In addition, oxidative vaporization reactions may be diffusion limited (refs. 12, 13, and 19). Experiments at different oxygen pressures and experiments with inert-gas additives (ref. 14) indicated that the oxidation was slightly diffusion limited for our experimental arrangement. The experimental conditions were dictated by the fast-flow, intermediate-pressure requirements of our studies of oxidation by oxygen atoms described in reference 17. The output of oxygen atoms optimized at an oxygen pressure of 15.3 N m^{-2} (0.115 torr) with a flow rate of 5×10^{-3} m^3 hr^{-1} (STP). Consequently, all the results reported herein were obtained at one pressure and one flow rate; namely, 15.3 N m^{-2} (0.115 torr) and 5×10^{-3} m^3 hr^{-1} (STP).

In order to obtain reaction-controlled rates, it was necessary to correct the measured rates. This was done by determining the escape fraction of the $CrO_3(g)$ formed in the oxidation reaction. In addition, the geometrical collection fraction for the apparatus was required. This fraction allowed correction for the fact that even in the absence of a boundary layer not all of the vapor product reaches the collection target (because of the finite size of target, shield, etc.). Both the escape fraction and the geometrical collection fraction were determined experimentally by using gold samples of the same width as the Cr-0.1Y samples.

The geometrical collection fraction was obtained by comparing the measured rate of evaporation of gold in a vacuum of 7×10^{-4} N m^{-2} ($\sim5\times10^{-6}$ torr) with the rate calculated from the vapor pressure data of reference 37. Two gold samples were used, and measurements were made at temperatures between 1273 and 1285 K. An average value of 0.455±0.05 was obtained for the geometrical collection fraction.

The escape fraction was obtained by comparing the measured rate of evaporation of gold in a vacuum of 7×10^{-4} N m^{-2} ($\sim5\times10^{-6}$ torr) with the rate measured under the conditions of the oxidation experiments, namely, 15.3 N m^{-2} (0.115 torr) of oxygen flowing at 5×10^{-3} m^3 hr^{-1} (STP). Numerous experiments yielded an average value of 0.335±0.04 for the escape fraction.

Reaction-controlled rates were calculated from our experimentally measured rate by dividing the measured rate by the product of the escape fraction and the geometrical collection fraction, namely, 0.153±0.03. The error we have associated with this product arises from the precision of our experiments and does not include errors arising from inaccuracies in the vapor pressure of gold. We estimate this inaccuracy to be as much as ±50 percent. Because of the magnitude of this possible error, we have not corrected our escape fraction for the fact that the atomic weight and other atomic parameters of gold are different from those of $CrO_3(g)$. Calculations indicate that the diffusivity of $CrO_3(g)$ is about 10 percent greater than the diffusivity of gold. In addition, we have assumed that the escape fraction is independent of the temperature of the sample. This assumption is based on the fact that for the oxidative vaporization of platinum the escape fraction was shown to be independent of sample temperature (ref. 14).

Analysis of Oxide Scale and Identification of Oxide Condensate

Numerous samples of our oxide scales were subjected to X-ray diffraction. The analyses always confirmed that the scale was Cr_2O_3.

Two samples were subjected to ion microprobe mass analysis:[4] one was unoxidized starting material and the other was a sample which had undergone several oxidative vaporization experiments. Yttrium was detected in the oxide layer of the reacted sample at a concentration approximately four times that detected in the bulk unoxidized sample. Samplings in different regions of the oxidized sample showed the yttrium content to vary by a factor of 5, while comparable data taken from the unoxidized sample showed the yttrium content to be constant. The spectrum obtained from the oxidized layer also revealed increases in the levels of all metallic contaminants, especially Fe, Al, Ca, and Mg. In addition, the elements Si, Mn, Na, and Co were identified as low-level metallic impurities. From these results it is concluded that the nonvolatile oxide-forming metallic impurities tend to concentrate in the surface oxide layer on the oxidized chromium where chromium has been lost by vaporization. However, because our oxide scales were generally removed between experiments, this effect should not have been cumulative and should not have affected our results.

The oxide condensate obtained in these experiments formed a reddish brown deposit on the platinum targets. When collected on polished platinum targets, the condensates were always readily soluble in water, forming yellow-colored solutions. If the platinum became etched (from cleaning in aqua regia), the deposits were often only partly soluble in water and required 1:1 HCl or fusion with $K_2S_2O_8$. For all the experiments reported herein only polished platinum targets were used, and the targets were cleaned with $K_2S_2O_8$. In addition, the oxide deposits were always dissolved as soon as feasible after a series of experiments.

Attempts to identify the deposits as CrO_3 by electron diffraction were unsuccessful and only Cr_2O_3 was identified. Apparently, the hydrocarbon background in the electron diffraction unit reduced the CrO_3 to Cr_2O_3. We have assumed that the deposits were $CrO_3(s)$ because of their reddish-brown color, their water solubility (Cr_2O_3 is insoluble in H_2O), the yellow color of the water solutions, the thermochemical predictions, and the findings of references 5 and 11.

Pressure Dependence

Experiments were performed to determine the order of the reaction with respect to the pressure of oxygen. Thermodynamic analysis indicates that the rate should depend

[4]Applied Research Laboratories, Sunland, California, provided the ion microprobe analyses.

on the 3/4 power of the oxygen pressure. Runs were made at a given temperature in which the total pressure and gas flow rate were maintained constant, and the oxygen partial pressure was varied by dilution with nitrogen gas. The oxygen pressures were varied from 15.3 to 9.33 N m^{-2} (0.115 to 0.070 torr). Greater dilution with nitrogen seemed to produce a permanent decrease in the rate of oxidation and resulted in an hysteresis effect with changing pressure. Nitrogen was used as the dilution gas because its molecular weight, collision cross section, and collision integral are nearly the same as those of oxygen. Thus, by keeping the total pressure of the O_2-N_2 mixture constant, the escape fraction should also remain constant. A log-log plot of our rates of oxidation as a function of the partial pressure of oxygen for a temperature of 1473 K is presented in figure 5. A line with a slope of 3/4 has been drawn through the points. It is evident that the rate obeys a 3/4 dependency on oxygen pressure within experimental precision.

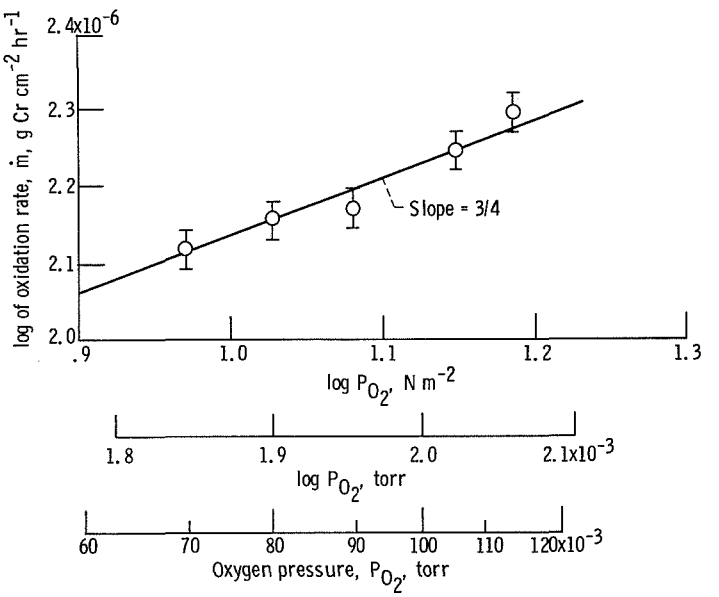

Figure 5. - Rate of oxidation as a function of partial pressure of oxygen. Temperature, 1473 K; total pressure, 15.3 N m^{-2} (0.115 torr); diluent gas, nitrogen.

Temperature Dependence

The effect of temperature on the oxidative vaporization was measured over the range 1270 to 1570 K at a constant oxygen pressure of 15.3 N m^{-2} (0.115 torr). Measurements at lower temperatures were impractical because of the unreasonably long times involved in collecting a measurable condensate. A typical set of results is shown in figure 6 in the form of an Arrhenius plot. The experimental rates, corrected for geometrical and diffusion-limitation factors, are represented by the circled data points.

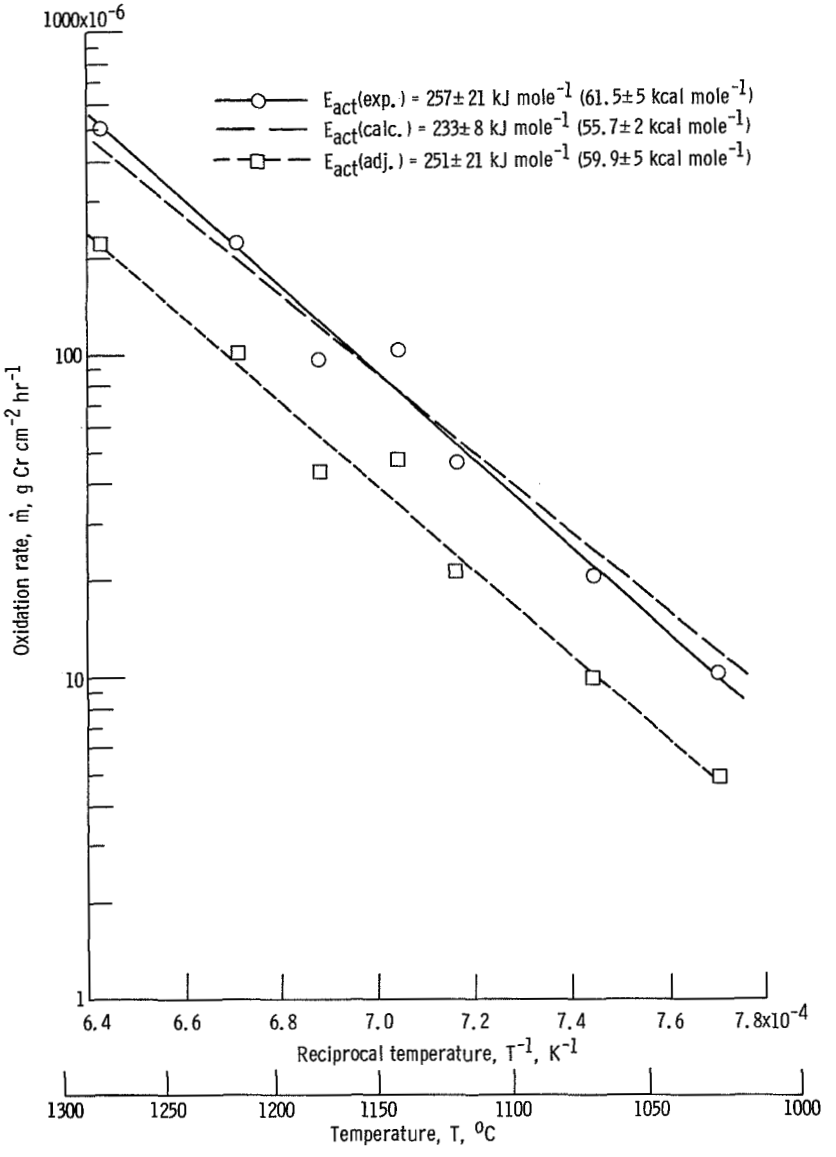

Figure 6. - Arrhenius plot of measured and calculated oxidation rates. Oxygen pressure, P_{O_2}, 15.3 N m^{-2} (0.115 torr).

The solid line through these points was derived from a least-squares fit of the data and yields an activation energy of 257±21 kJ $mole^{-1}$ (61.5±5 kcal $mole^{-1}$) for the oxidation process.

We have extensively investigated the effect of varying several experimental parameters on the value obtained for the activation energy. Parameters varied included sample, oxygen pressure (6.67, 10.0, and 15.3 N m^{-2} (0.050, 0.075, and 0.115 torr)), flow rate (2 and 5×10^{-3} m^3 hr^{-1} (STP)), sample-target separation (1.8 to 3.0 cm), and sample composition (Cr-0.1Y and Ni-40 Cr). Although the actual rates varied with some of these parameters, the temperature dependence did not and the energy of activa-

tion was found to be the same within an experimental precision of ±21 kJ $mole^{-1}$ (±5 kcal $mole^{-1}$).

Included in figure 6, as the dashed line, are the predicted rates calculated from equation (3) for a pressure of 15.3 N m^{-2} (0.115 torr). As noted previously, the experimental energy of activation and the enthalpy of reaction may be expected to be numerically equal for oxidative vaporization reactions of the type being considered. Actually, the two quantities differ by a small amount because of a temperature term that arises from the Hertz-Langmuir equation. The energy of activation can be calculated from the enthalpy of the reaction by the relation (ref. 38)

$$\frac{E_{act}}{R} = \frac{\Delta H^{o}_{T}}{R} - \frac{T}{2} \tag{4}$$

The enthalpy in this temperature range is ΔH^{o}_{1400} = 238 kJ $mole^{-1}$ (57.1 kcal $mole^{-1}$). Thus, the calculated energy of activation is 233 kJ $mole^{-1}$ (55.7 kcal $mole^{-1}$) as given in figure 6.

The experimental rates are not exactly comparable to the rates calculated from thermodynamic data because the temperature of the oxygen in our experiments is not at the temperature of the specimen. In fact, it is probably closer to room temperature.[5] In order to facilitate comparison, we have adjusted our experimental rates by multiplying by the factor[6] $(300/T)^{1/2}$, where room temperature has been taken as 300 K. These adjusted results are given as the squared data points in figure 6. The line through these points was derived from a least-squares fit and yields an "adjusted" energy of activation of 251±21 kJ $mole^{-1}$ (59.9±5 kcal $mole^{-1}$). This value is in agreement with our calculated value of 233±8 kJ $mole^{-1}$ (55.7±2 kcal $mole^{-1}$) within experimental error. The rates represented by the squared data points are roughly one-half of the calculated rates.

---

[5]The quantity of importance in experiments involving gas-solid reactions is the collision flux of the gas with the solid. This depends on the pressure and the temperature of the gas. When a small-diameter filament is heated in a bulb containing gas at a pressure low enough that the mean free path is comparable to the diameter of the bulb (Knudsen region), all the gas molecules striking the wire have a temperature equal to that of the bulb. As the pressure is increased and/or the diameter of the wire is increased, the gas molecules striking the wire will have temperatures approaching the wire temperature. In the viscoelastic pressure region, one usually takes the gas temperature in the boundary layer as the average of the wire and bulb temperature. In our experiments the ratio of the mean free path to the ribbon width was about 0.2. While this is not in the Knudsen region, is is fairly close, and for the sake of simplicity we have assumed that the gas striking the chromium ribbon is at room temperature.

[6]The collision flux Z varies as $T^{-1/2}$ as indicated by the well-known kinetic theory equation $Z = P(2\pi MRT)^{-1/2}$.

This is probably within the experimental error of our measurements, which depends directly on the accuracy with which we could measure the vaporization rate of gold in our apparatus. In addition, we have probably underestimated the temperature of the gas in the boundary layer (see footnote 5 on p. 15). If so, the adjusted rates may have been reduced too much, and a value closer to the experimental rates may be more accurate. In any case, the agreement is quite good for this type of measurement.

Theoretical Rate Equation

We have shown that the kinetics of the oxidative vaporization of $Cr_2O_3(s)$ in the reaction-controlled region can be adequately described by the equilibrium thermodynamic data. It is, therefore, possible to derive an equation for the rate of oxidative vaporization in any pressure region under various flow conditions. Only the equilibrium constant of the reaction and the Nusselt number obtained from dimensionless fluid correlations are required. The development parallels that of Bartlett (refs. 15 and 16).

The oxidation process is represented by the reaction

$$\frac{1}{2}Cr_2O_3(s) + \frac{3}{4}O_2(g) \underset{k_b}{\overset{k_f}{\rightleftharpoons}} CrO_3(g) \tag{5}$$

At pressures where the mean free path λ of the $CrO_3(g)$ is large compared with the width L of the chromium ribbon, all the $CrO_3(g)$ formed escapes from the ribbon and the rate is reaction controlled. At higher pressures where $\lambda/L < 1$, some of the volatilizing $CrO_3(g)$ will be reflected back to the chromium ribbon, where it will decompose; and the rate will be diffusion limited. In this case, the rate will be determined by the rate of mass transport of $CrO_3(g)$ through a stagnant boundary layer of oxygen (because $P_{CrO_3} << P_{O_2}$). The mass flux of $CrO_3(g)$ across the boundary layer is given by

$$\dot{m}_D = \frac{k_m M_{CrO_3}\left(P_{CrO_3,s} - P_{CrO_3,\delta}\right)}{P_t} \tag{6}$$

where $\dot{m}_D$ is in g cm^{-2} sec^{-1}; k_m is the mass transfer coefficient which can be calculated from boundary-layer theory (mole cm^{-2} sec^{-1}); $P_{CrO_3,s}$ and $P_{CrO_3,\delta}$ are the steady-state values of the partial pressures of $CrO_3(g)$ at the surface of the chromium ribbon and at the outer edge of the boundary layer, respectively; and P_t is the

total pressure or the stagnation pressure in a flowing system. Generally, $P_{CrO_3,\delta} = 0$ and equation (6) reduces to

$$\dot{m}_D = \frac{k_m M_{CrO_3} P_{CrO_3,s}}{P_t} \tag{7}$$

The rate of formation of $CrO_3(g)$ by chemical reaction is given by

$$\dot{m}_R = M_{CrO_3}\left(k_f P_{O_2,s}^{3/4} - k_b P_{CrO_3,s}\right) \tag{8}$$

where k_f and k_b are the forward and backward rate constants of the reaction, respectively; and $P_{O_2,s}$ is the partial pressure of oxygen at the surface of the chromium ribbon. However, because $P_{CrO_3(g)} << P_{O_2}$, $P_{O_2,s}$ can be taken equal to the pressure in the system: P_{O_2}. We have tacitly assumed in equation (8) that the condensation coefficient of $CrO_3(g)$ on the chromium is 1.

The exact value of $P_{CrO_3,s}$ is unknown. However, it can be eliminated from equations (7) and (8). In addition, from consideration of the mass balance, $\dot{m}_D = \dot{m}_R$, and by definition, $K_e = k_f/k_b$. Performing these operations and substitutions, we obtain

$$\dot{m}_D = \frac{M_{CrO_3} k_b K_e P_{O_2}^{3/4}}{1 + k_b \frac{P_t}{k_m}} \tag{9}$$

The backward rate constant k_b is simply the surface collision frequency of $CrO_3(g)$ molecules in mole cm^{-2} sec^{-1} per unit pressure and is given by the kinetic theory expression

$$k_b = \left(2\pi M_{CrO_3} RT\right)^{-1/2} \tag{10}$$

Inserting this expression into equation (9), we obtain

$$\dot{m}_D = \frac{\left(2\pi M_{CrO_3} RT\right)^{-1/2} M_{CrO_3} K_e P_{O_2}^{3/4}}{1 + \left(2\pi M_{CrO_3} RT\right)^{-1/2} \frac{P_t}{k_m}} \tag{11}$$

where R is in erg mole^{-1} K^{-1} and P is in dyne cm^{-2}.

Equation (11) is valid at all pressures and at temperatures for which reaction (5) occurs. At low pressures where $1 >> \left(2\pi M_{CrO_3} RT\right)^{-1/2} (P_t/k_m)$, equation (11) reduces to

$$\dot{m}_D = \left(2\pi M_{CrO_3} RT\right)^{-1/2} M_{CrO_3} K_e P_{O_2}^{3/4} \tag{12}$$

which is analogous to equation (3) except it is in units of g CrO_3(g) rather than g Cr. The rate of oxidation is proportional to $P_{O_2}^{3/4}$ and is reaction controlled. At high pressures where $1 << \left(2\pi M_{CrO_3} RT\right)^{-1/2} (P_t/k_m)$, equation (11) reduces to

$$\dot{m}_D = \frac{M_{CrO_3} k_m K_e P_{O_2}^{3/4}}{P_t} \tag{13}$$

The mass transfer coefficient k_m is related to the Nusselt number Nu_m for mass transfer by the relation

$$k_m = \frac{Nu_m P_t D_{CrO_3}}{LRT_g} \tag{14}$$

where D_{CrO_3} is the diffusion coefficient of CrO_3 in cm^2 sec^{-1} and L is a characteristic dimension of the sample (i.e., the ribbon width). All the quantities in these two equations, (13) and (14), are known except the diffusion coefficient and the Nusselt number. The diffusion coefficient can be calculated from the Chapman-Enskog equation, and

the Nusselt number is obtained from semiempirical correlations used extensively in engineering analyses (ref. 39).

CONCLUSIONS

Experimental rates for the oxidative vaporization of Cr_2O_3 in low-pressure, flowing oxygen, when corrected for geometrical and diffusion-limiting factors, agree within experimental error with rates calculated from equilibrium thermodynamic data.

The experimentally determined pressure and temperature dependencies also agree within experimental error with the dependencies predicted from equilibrium thermodynamic data. Both experiment and thermodynamic data show that the reaction varies as the 3/4 power of the oxygen pressure. The experimental energy of activation, adjusted for the fact that the oxygen is not at the temperature of the specimen, was 251 kJ $mole^{-1}$ (59.9±5 kcal $mole^{-1}$) and the enthalpy calculated for the reaction was 233 kJ $mole^{-1}$ (55.7±2 kcal $mole^{-1}$).

Thus, we can conclude, from these findings, that the rate of oxidative vaporization of Cr_2O_3 in oxygen can be calculated realistically from equilibrium thermodynamic data. An equation is derived for calculating the rate under any conditions of temperature, pressure, and flow condition by using thermodynamic data and the Nusselt number obtained from dimensionless fluid correlations.

Lewis Research Center,
National Aeronautics and Space Administration,
Cleveland, Ohio, January 11, 1974,
502-01.

REFERENCES

1. Wallwork, G. R.; and Hed, A. Z.: The Oxidation of Ni-20 wt. % Cr-2ThO_2. Oxidation of Metals, vol. 3, no. 3, 1971, pp. 229-241.

2. Lowell, Carl E.; Deadmore, Daniel L.; Grisaffe, Salvatore J.; and Drell, Isadore L.: Oxidation of Ni-20Cr-2ThO_2 and Ni-30Cr-1.5Si at 800°, 1000°, and 1200° C. NASA TN D-6290, 1971.

3. Hagel, William C.: Factors Controlling the High-Temperature Oxidation of Chromium. Trans. ASM, vol. 56, 1963, pp. 583-599.

4. Seltzer, M. S.; Wilcox, B. A.; and Stringer, J.: The Oxidation Behavior of Ni-Cr-Al-2ThO_2 Alloys at 1093° and 1204° C. Met. Trans., vol. 3, no. 9, Sept. 1972, pp. 2391-2401.

5. Caplan, D.; and Cohen, M.: The Volatilization of Chromium Oxide. J. Electrochem. Soc., vol. 108, no. 5, May 1961, pp. 438-442.

6. Cadiou, L.; and Paidassi, J.: Contribution to the Study of the Reaction of Chromium with Oxygen at High Temperatures. Memoires Scientifiques Rev. Metallurg., vol. 66, No. 3, 1969, pp. 217-225.

7. Stringer, J.: The Functional Form of Rate Curves for the High-Temperature Oxidation of Dispersion-Containing Alloys Forming Cr_2O_3 Scales. Oxidation of Metal, vol. 5, No. 10, Oct. 1972, pp. 49-58.

8. Giggins, C. S.; and Pettit, F. S.: The Oxidation of TD-NiC (Ni-20Cr-2 vol pct ThO_2) Between 900° and 1200° C. Met. Trans., vol. 2, No. 4, Apr. 1971, pp. 1071-1078.

9. Tedmon, C. S., Jr.: The Effect of Oxide Volatilization on the Oxidation Kinetics of Cr and Fe-Cr Alloys. J. Electrochem. Soc., vol. 113, No. 8, Aug. 1966, pp. 766-768.

10. Graham, H. C.; and Davis, H. H.: Oxidation/Vaporization Kinetics of Cr_2O_3. J. Am. Ceram. Soc., vol. 54, No. 2, Feb. 1971, pp. 89-93.

11. Grimley, R. T.; Burns, R. P.; and Inghram, Mark G.: Thermodynamics of the Vaporization of Cr_2O_3: Dissociation Energies of CrO, CrO_2, and CrO_3. J. Chem. Phys., vol. 34, No. 2, Feb. 1961, pp. 664-667.

12. Fryburg, George C.; and Murphy, Helen M.: On the Use of Furnaces in the Measurement of the Rate of Oxidation of Platinum and Other Metals Forming Volatile Oxide. Trans. AIME, vol. 212, No. 5, Oct. 1958, pp. 660-661.

13. Fryburg, George C.; and Petrus, Helen M.: Kinetics of the Oxidation of Platinum. J. Electrochem. Soc., vol. 108, No. 6, June 1961, pp. 496-503.

14. Fryburg, George C.: The Pressure Dependency in the Oxidation of Platinum Explained by a Boundary-Layer Diffusion Mechanism. Trans. AIME, vol. 233, No. 12, Nov. 1965, pp. 1986-1989.

15. Bartlett, R. W.: Platinum Oxidation Kinetics with Convective Diffusion and Surface Reaction. J. Electrochem. Soc., vol. 114, no. 6, June 1967, pp. 547-550.

16. Bartlett, R. W.: Tungsten Oxidation Kinetics at High Temperatures. Trans. AIME, vol. 230, no. 8, Aug. 1964, pp. 1097-1103.

17. Fryburg, George C.; Kohl, Fred J.; and Stearns, Carl A.: Enhancement of Oxidative Vaporization of Chromium (III) Oxide and Chromium by Oxygen Atoms. NASA TN D-7629, 1974.

18. Smithells, Colin J., ed.: Metal Reference Book. First ed., Butterworths Sci. Pub., 1949.

19. Rosner, D. E.: High-Temperature Gas-Solid Reactions. In Annual Review of Materials Science Vol. 2, R. A. Huggins, ed., Annual Reviews Inc., 1972, pp. 573-606.

20. Kellogg, H. H.: Vaporization Chemistry in Extractive Metallurgy. Trans. AIME, vol. 236, no. 5, May 1966, pp. 602-615.

21. Jansson, S. A.; and Gulbransen, E. A.: Evaluation of Gas Metal Reactions by Means of Thermochemical Diagrams. Extended Abstracts of the 4th International Congress on Metallic Corrosion, Amsterdam, Netherlands, Sept. 7-14, 1969, p. 77.

22. Gulbransen, Earl A.; and Jansson, Sven A.: Vaporization Chemistry in the Oxidation of Carbon, Silicon, Chromium, Molybdenum and Niobium. Heterogeneous Kinetics at Elevated Temperatures. G. R. Belton and W. L. Worrell, eds., Plenum Press, 1970, pp. 181-208.

23. Jansson, Sven A.: Thermochemistry of Liquid Metal-Gas Crucible Reactions in Vacuum. J. Vac. Sci. and Tech., vol. 7, no. 6, Nov.-Dec. 1970, pp. 55-513.

24. Gulbransen, Earl A.; and Jansson, Sven A.: Thermochemistry of Gas-Metal Reactions. Ch. 4 in Oxidation of Metals and Alloys, American Society for Metals, 1971.

25. Schick, H. L., ed.: Thermodynamics of Certain Refractory Compounds. Academic Press, 1966.

26. Kim, Y.: Volatilization of Chromic Oxide in Oxygen and Water Vapor. Ph.D. Thesis, Univ. Pennsylvania, 1969. G. R. Belton, advisor.

27. Kohl, Fred J.; and Stearns, Carl A.: Vaporization of Chromium Oxides from the Surface of TD NiCr Under Oxidizing Conditions. NASA TM X-52879, 1970.

28. Kohl, Fred J.; and Stearns, Carl A.: Oxidation/Vaporization of Silicide Coated Columbium Base Alloys. NASA TM X-67980, 1971.

29. Schäefer, Harold; and Rinke, Klaus: Gaseous Chromium(VI)Oxide by Mass Spectroscopy. Z. Naturforschung, Sec. B, No. 7, 1965, pp. 702-703.

30. McDonald, J. D.; and Margrave, J. L.: Mass Spectrometric Studies at High Temperatures XVI. Sublimation and Vaporization of Chromium Trioxide. J. Inorg. Nucl. Chem., vol. 30, No. 2, Feb. 1968, pp. 665-667.

31. Washburn, C. A.: A Mass Spectrometric Study of the Sublimation of Chromium Trioxide. Ph.D. Thesis, Univ. of California (UCRL-18685), 1969.

32. Kant, Arthur; and Strauss, Bernard: Dissociation Energy of Cr_2. J. Chem. Phys., vol. 45, No. 8, Oct. 15, 1966, pp. 3161-3162.

33. Wicks, C. E.; and Block, F. E.: Thermodynamic Properties of 65 Elements - Their Oxides, Halides, Carbides and Nitrides. Bull. 605, U.S. Bureau of Mines, 1963.

34. Gulbransen, Earl A.: Thermochemistry and the Oxidation of Refractory Metals at High Temperature. Corrosion, vol. 26, No. 1, Jan. 1970, pp. 19-28.

35. Schwartz, Robert S.; Fankuchen, I.; and Ward, Ronald: The Products of Thermal Decomposition of Chromium Trioxide. J. Amer. Chem. Soc., vol. 74, Apr. 5, 1972, pp. 1676-1677.

36. Rapp, R. A.: Vaporization Losses from Cr_2O_3 Protective Scales. In High Temperature Corrosion of Aerospace Alloys, AGARD-CP-120, 1973, pp. 147-154.

37. Hultgren, Ralph; Desai, Pramod D.; Hawkins, Donald T.; Gleiser, Molly; Kelley, Kenneth K.; and Wagman, Donald D.: Selected Values of the Thermodynamic Properties of the Elements. American Society for Metals, 1973, p. 47.

38. Rutner, Emile: Some Limitations of the Use of the Langmuir and Knudsen Techniques for Determining Kinetics of Evaporation. In Condensation and Evaporation of Solids, Emile Rutner, P. Goldfinger, and J. P. Hirth, eds., Gordon and Beach, 1962, pp. 149-163.

39. Bird, R. Byron; Stewart, Warren E.; and Lightfoot, Edwin N.: Interphase Transport in Multicomponent Systems. Ch. 21 in Transport Phenomena. John Wiley & Sons, Inc., 1960.

NATIONAL AERONAUTICS AND SPACE ADMINISTRATION
WASHINGTON, D.C. 20546

OFFICIAL BUSINESS
PENALTY FOR PRIVATE USE $300

SPECIAL FOURTH-CLASS RATE BOOK

POSTAGE AND FEES PAID
NATIONAL AERONAUTICS AND SPACE ADMINISTRATION
451

U.S.MAIL

POSTMASTER: If Undeliverable (Section 158 Postal Manual) Do Not Return

"The aeronautical and space activities of the United States shall be conducted so as to contribute . . . to the expansion of human knowledge of phenomena in the atmosphere and space. The Administration shall provide for the widest practicable and appropriate dissemination of information concerning its activities and the results thereof."

—NATIONAL AERONAUTICS AND SPACE ACT OF 1958

NASA SCIENTIFIC AND TECHNICAL PUBLICATIONS

TECHNICAL REPORTS: Scientific and technical information considered important, complete, and a lasting contribution to existing knowledge.

TECHNICAL NOTES: Information less broad in scope but nevertheless of importance as a contribution to existing knowledge.

TECHNICAL MEMORANDUMS: Information receiving limited distribution because of preliminary data, security classification, or other reasons. Also includes conference proceedings with either limited or unlimited distribution.

CONTRACTOR REPORTS: Scientific and technical information generated under a NASA contract or grant and considered an important contribution to existing knowledge.

TECHNICAL TRANSLATIONS: Information published in a foreign language considered to merit NASA distribution in English.

SPECIAL PUBLICATIONS: Information derived from or of value to NASA activities. Publications include final reports of major projects, monographs, data compilations, handbooks, sourcebooks, and special bibliographies.

TECHNOLOGY UTILIZATION PUBLICATIONS: Information on technology used by NASA that may be of particular interest in commercial and other non-aerospace applications. Publications include Tech Briefs, Technology Utilization Reports and Technology Surveys.

Details on the availability of these publications may be obtained from:

SCIENTIFIC AND TECHNICAL INFORMATION OFFICE

NATIONAL AERONAUTICS AND SPACE ADMINISTRATION

Washington, D.C. 20546